J. Membrane Biol. 92, 9–19 (1986)

The Journal of
Membrane Biology

Membrane Electrical Parameters in Turtle Bladder Measured Using Impedance-Analysis Techniques

Chris Clausen† and Troy E. Dixon‡

† Department of Physiology and Biophysics, SUNY Health Sciences Center, Stony Brook, New York 11794-8661
and ‡ Department of Medicine, VA Medical Center, Northport, New York 11768

Summary. Equivalent-circuit impedance analysis experiments were performed on the urinary bladders of freshwater turtles in order to quantify membrane ionic conductances and areas, and to investigate how changes in these parameters are associated with changes in the rate of proton secretion in this tissue. In all experiments, sodium reabsorption was inhibited thereby unmasking the electrogenic proton secretion process. We report the following: (1) transepithelial impedance is represented exceptionally well by a simple equivalent-circuit model, which results in estimates of the apical and basolateral membrane ionic conductances and capacitances; (2) when sodium transport is inhibited with mucosal amiloride and serosal ouabain, the apical and basolateral membrane conductances and capacitances exhibit a continual decline with time; (3) this decline in the membrane parameters is most likely caused by subtle time-dependent changes in cell volume, resulting in changes in the areas of the apical and basolateral membranes; (4) stable membrane parameters are obtained if the tissue is not treated with ouabain, and if the oncotic pressure of the serosal solution is increased by the addition of 2% albumin; (5) inhibition of proton secretion using acetazolamide in CO_2 and HCO_3^--free bathing solutions results in a decrease in the area of the apical membrane, with no significant change in its specific conductance; (6) stimulation of proton transport with CO_2 and HCO_3^--containing serosal solution results in an increase in the apical membrane area and specific conductance. These results show that our methods can be used to measure changes in the membrane electrophysiological parameters that are related to changes in the rate of proton transport. Notably, they can be used to quantify in the live tissue, changes in membrane area resulting from changes in the net rates of endocytosis and exocytosis which are postulated to be intimately involved in the regulation of proton transport.

Key Words proton transport · turtle bladder · equivalent-circuit analysis · impedance analysis · cell volume regulation · endocytosis · exocytosis

Introduction

In the urinary bladder of freshwater turtles, protons are secreted electrogenically in a manner analogous to acid secretion by the collecting tubule of the kidney. Recent evidence suggests that one means of regulating the rate of proton transport involves altering the number of proton pumps present in the apical membrane. Proton pump-containing vesicles located in the cytoplasm of the mitochondria-rich cells are seen to undergo exocytotic fusion with the apical membrane when transport is stimulated with CO_2 (Gluck et al., 1982). Conversely, inhibition of proton transport achieved by removal of CO_2 is associated with an increased rate of endocytotic removal of proton pump-containing membrane leading to an increase in the number of intracellular vesicles (Reeves, Gluck & Al-Awqati, 1982). These findings support the notion that membrane-shuttling mechanisms contribute to the regulation of proton transport in this epithelium by altering the number of proton pumps present in the apical membrane.

In order to obtain a change in the number of pumps in the apical membrane, one would need to realize a net difference between changes in the rates of endocytosis and exocytosis. If all vesicles contain roughly the same density of pumps, then changes in these net rates should be reflected in changes in the area of the apical membrane. Indeed, morphometric analyses have shown that stimulation of transport by CO_2 results in an increase in apical membrane area, concomitant with a decrease in the number of cytoplasmic vesicles (Stetson & Steinmetz, 1983). In order to make a cogent argument about the role played by membrane-shuttling events in the regulation of proton transport, one should be able to show that the temporal relationship between the changes in the rate of transport and surface area also support the hypothesis. However, it is difficult to study this using morphometric analyses of fixed tissues.

In order to study changes in membrane area in the live tissue, we have been analyzing transepithelial impedance using equivalent-circuit techniques. Impedance analysis has been widely used in the analysis of the electrical properties of a variety of

epithelia (*see* Diamond & Machen, 1983, for a recent review), and is capable of measuring the different membrane ionic conductances, as well as their respective electrical capacitances. Membrane capacitance has been shown to be directly proportional to membrane area, and hence can be used as a measure of the areas, since biological membrane-specific capacitance has been found to be remarkably constant at approximately 1 $\mu F/cm^2$ (Cole, 1972). Since impedance analysis is a noninvasive technique which allows the rapid and repeated measurement of the different epithelial membrane electrical properties, we hoped to be able to quantify changes in membrane areas, as well as conductances, and to relate these changes to changes in the rate of proton transport.

Development of a suitable equivalent circuit model for use in these studies required that we take into consideration the known morphological and physiological characteristics of the bladder. This epithelium is known to have two predominant cell types (Rosen, 1970). Granular cells account for roughly 75% of the population and are thought to mediate sodium transport, whereas mitochondria-rich cells, which represent 10 to 20% of the population, are thought to be responsible for proton transport (Schwartz et al., 1982). Thus, the presence of a heterogenous population of cells with different transport properties presents a potential problem in trying to use transepithelial measurements to follow membrane electrical characteristics of the minority cell type.

In this paper we report the use of impedance analysis to characterize the electrical properties of the turtle bladder. We demonstrate that the stability of the base-line conductance and capacitance values are critically dependent upon the initial incubation conditions. Notably, we report findings which suggest a relationship between cell volume and membrane surface area. We subsequently show how the membrane electrical parameters change in response to maneuvers which alter the rate of proton transport, using CO_2 as a stimulator, and 4-acetamido-4-isothiocyano-stilbene-2,2-disulfonic acid (SITS) or acetazolamide (AZ) as inhibitors. The results demonstrate that this approach can be used to monitor concurrently the rate of transport, the membrane ionic conductances, and the morphological state of the tissue, as reflected by the different membrane areas. Moreover, the results support the notion that changes in the membrane electrical characteristics of the mitochondria-rich cell type can be sensitively measured by use of transepithelial impedance analysis.

Materials and Methods

Dissection, Chamber, and Solutions

Freshwater turtles *Pseudymys scripta elegans* were double pithed, and the urinary bladders were removed with a minimal amount of handling. Hemibladders were then mounted in a modified Ussing chamber specially designed to eliminate edge damage (Lewis et al., 1977). Nominal chamber area was 2.0 cm^2, and each half-chamber had a volume of 15 ml. The mucosal and serosal solutions were bubbled continuously and gently stirred using magnetic fleas. All experiments were carried out at room temperature.

In most experiments, the mucosa and serosa were bathed in a modified Ringer's solution (control solution) containing (in mM): 100 NaCl, 3.5 KCl, 1.0 $MgCl_2$, 1.0 $CaCl_2$, 1.0 NaH_2PO_4, 1.5 Na_2HPO_4, and 5.0 D-glucose. The pH was adjusted to 7.0, and the chambers were bubbled with room air which had been passed through KOH traps to remove CO_2. In some experiments where proton transport was enhanced with CO_2, the above solution was modified to contain 100 mM NaCl and 10 mM $NaHCO_3$, and was subsequently bubbled with a gas mixture containing 5% CO_2 and 95% air. After equilibration with the gas mixture, the pH was verified to be 7.0.

To inhibit proton transport, 0.5 mM SITS (Polyscience, Worthington, Pa.) or 50 μM AZ (Sigma, St. Louis, Mo.) was added to the serosal solution. 0.5 mM SITS acts irreversibly, but 50 μM AZ is reversible, as has been previously reported (Schwartz et al., 1972).

Oncotic Pressure and Cell Volume Changes

Two percent bovine serum albumin (Fraction V, Sigma) was added to the serosal solution in some experiments in order to alter the oncotic pressure. In these cases, a small amount of silicon oil (Antifoam A spray, Dow Corning, Midland, Mich.) was sprayed on the surface of the serosal solution in order to prevent foam production caused by bubbling in the presence of the albumin.

Cell swelling was induced in some experiments by the mucosal addition of 20 to 100 U/ml nystatin (Sigma) disolved in microliter aliquots of methanol.

Electrical Measurements

Transepithelial voltage (V_t) was measured differentially using a high-speed high-impedance amplifier (Model 113, Princeton Applied Research, Princeton, N.J.), connected to a pair of Ag/AgCl electrodes mounted close to the preparation. A second set of Ag/AgCl electrodes was mounted at opposite ends of the chamber and was used to pass transepithelial current. Constant current was generated using a calibrated 1 MΩ carbon series resistor connected to the mucosal electrode; the serosal current electrode was connected to ground. The short-circuit current (I_{sc}) was measured intermittently by passing a 500-msec current pulse which depolarized V_t to zero. A positive current is defined as one flowing from mucosa to serosa.

Transepithelial Impedance Measurements

Transepithelial impedance was measured using the method of Clausen and Fernandez (1981), as detailed in Clausen et al. (1986). Briefly, a wide-band pseudorandom binary signal was generated digitally and converted to a constant transepithelial current of 14 μA/cm^2 (peak-to-peak). The resulting transepithelial voltage response was amplified, filtered by an antialiasing filter, digitized, and recorded by computer. The impedance was calculated by dividing the cross-spectral density of the voltage and the current by the power-spectral density of the applied current. Two digitization bandwidths were used to provide good low- and high-frequency resolution. In addition, signal averaging was used to improve the signal-to-noise ratio. Total data acquisition time was less than 5 sec per run and resulted in *ca.* 400 data points linearly spaced in frequency from 2.2 to 860 Hz, and an equal number of points linearly spaced in frequency from 22 Hz to 8.6 kHz. These data were subsequently merged and reduced to 100 data points (actually 200 numbers since each data point consists of a phase angle and impedance magnitude measurement) logarithmically spaced in frequency from 2.2 Hz to 8.6 kHz.

The impedance was represented as Bode plots, which plot phase angle and log impedance magnitude against frequency. These data were then fitted by a morphologically based equivalent-circuit model (*see* Results) composed of resistors and capacitors that correspond analogously to the different membrane ionic conductances and capacitances (proportional to area), respectively. This was accomplished using a nonlinear least-squares curve-fitting algorithm. After each curve fit, the Hamilton R-factor was computed as an objective measure of fit; the R-factor can be interpreted as the average percent misfit between the model and the data. We also computed estimates of the best-fit parameter standard deviations, but since these result from a linearization of the model about the best-fit parameter set, they cannot be used to provide a confidence interval for each parameter. However, if a standard deviation exceeded 10% of the parameter value, that parameter was considered poorly determined by the available data. The complete details of the curve fitting and statistical computations can be found in Clausen et al. (1979), with subsequent modifications described in Clausen et al. (1986).

Measurement of Proton Secretion Rate

The bladder possesses an electrogenic sodium reabsorption process which complicates the measurement of electrogenic proton secretion using the voltage-clamp technique. In order to eliminate sodium reabsorption, all experiments were performed in the presence of 0.1 mM mucosal amiloride (kindly provided by Merck, Sharp and Dohme, Rahway, N.J.), and in a few experiments, 1 mM serosal ouabain (Sigma). Prior to the application of amiloride or ouabain, V_t is negative on the mucosal side, reflecting primarily sodium reabsorption. The application of amiloride or ouabain results in a rapid reversal of the polarity of the transepithelial potential, thereby unmasking the concomitant electrogenic proton secretion. I_{sc} was then measured and was interpreted as reflecting the rate of proton secretion, as confirmed previously using pH-stat techniques (Steinmetz, 1974). We should note that under these conditions, I_{sc} is commonly referred to as the reverse short-circuit current, or RSCC.

Results

Equivalent-Circuit Model

To be able to analyze quantitatively the measured data requires a morphologically based equivalent-circuit model comprising resistors and capacitors that correspond analogously to the different membranes. The simplest such model appropriate for urinary bladder epithelium is a so-called lumped model (*see* Clausen et al., 1979). In this model, the apical membrane is represented as a parallel resistor-capacitor (RC) circuit, where the resistor ($R_a = 1/G_a$) represents the ionic conductance of the apical membrane, and the capacitor (C_a) represents the apical membrane capacitance and is proportional to membrane area. Another RC circuit in series with this circuit is then added to represent the electrical properties of the basolateral membrane, where the membrane circuit elements ($R_b = 1/G_b$, and C_b) have analogous interpretations. The paracellular pathway for current flow, comprising the tight junctions and lateral spaces, is represented as a parallel resistor ($R_j = 1/G_j$). Due to the small surface area of the tight junctions compared with the apical membrane area, the capacitance of the junctions is considered negligible. Finally, a small series resistor (R_s) is added to represent the finite resistance between the voltage electrodes and the epithelial surfaces.

Clausen et al. (1979), in their studies of mammalian urinary bladder, found that the lumped model was incapable of representing accurately the measured impedance, and we also found this to be the case in the turtle bladder. Due to the narrow width (*ca.* 10 mm) of the lateral spaces, and their relatively long and tortuous path length (*ca.* 20 μm), a significant series resistance is expected to be distributed along the lateral membrane, and is shown schematically in Fig. 1. Calculations show that this resistance will become comparable to the basolateral membrane impedance magnitude at high frequencies. We therefore used the distributed model originally derived by Clausen et al. (1979) and subsequently simplified in Clausen et al. (1986). The model requires an additional circuit parameter R_p which describes the path resistance of the lateral spaces.

Clausen et al. (1979) also showed that the circuit parameters of the distributed model were not completely independent, since the distributed model is virtually identical to a simpler model containing no paracellular electrical pathway ($G_j = 0$). In essence, G_j mathematically lumps into the other

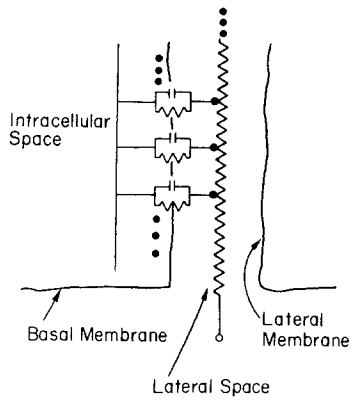

Fig. 1. Schematic representation of the impedance of the basolateral membrane and lateral spaces. The path resistance R_P of the lateral spaces forms a distributed impedance with the basolateral membrane

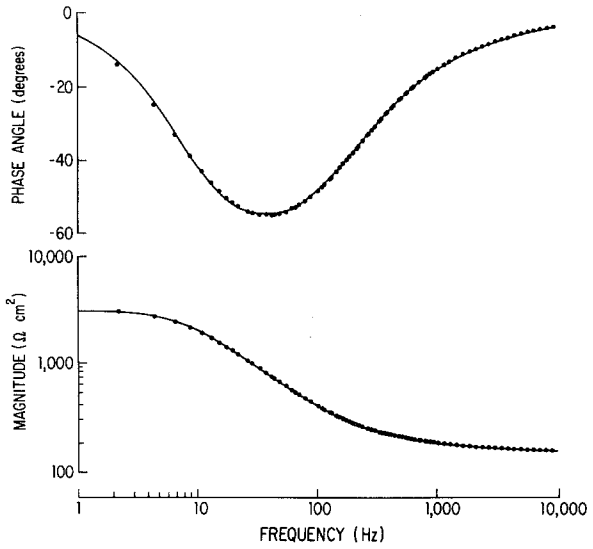

Fig. 2. Measured impedance (symbols) fitted by the distributed model (lines) from a representative impedance run. The good agreement between the model and the measured data is typical

parameters. In all fits of the measured impedance by the distributed model, G_j was tacitly assumed to be negligible compared to the transcellular conductance, but this assumption was subsequently justified as being reasonable (*see below*).

Figure 2 shows measured impedance (symbols) from a randomly chosen impedance run. The curves drawn through the data show the model-predicted impedance derived from fitting the distributed model to the data. The agreement between the model and the data is typical, resulting in an R-factor of 0.70%. The mean R-factor for 100 different runs was 0.88 ± 0.02% (SEM). We rejected two runs which, for unexplained reasons, exhibited R-factors of greater than 1.5%. An R-factor of 1.5% is more than three standard deviations higher than the mean value.

Paracellular Conductance

We have not yet justified the earlier assumption that G_j is small compared to the transcellular conductance pathway, hence two questions must be addressed. Is G_j truly negligible? If not, can we determine accurately the other membrane parameters using the distributed model?

Clausen and Wills (1981) showed that estimates of membrane resistance ratios (α) or voltage-divider ratios (fR_a) derived from the impedance analysis should be equivalent to microelectrode-determined values only if G_j is small compared to the transcellular conductance. Notably, if G_j is comparable to the transcellular conductance, then the impedance-predicted values will be higher than values obtained from microelectrode studies.

For an epithelium possessing a nonnegligible lateral-space resistance, the voltage drop across the basolateral membrane resulting from an applied transepithelial current is dependent not only on R_b but also on R_p. Hence in order to compare our estimates of α and fR_a with values determined using microelectrode studies, we define an effective basolateral resistance (R'_b) which explicitly considers effects due to the distributed resistance of the lateral spaces. R'_b is derived directly from the distributed model and is given by:

$$R'_b = \sqrt{R_b R_p} \coth \sqrt{R_p/R_b}. \quad (1)$$

α and fR_a are then defined as R_a/R'_b, and $R_a/(R_a + R'_b)$, respectively.

Under control conditions (hemibladders bathed in phosphate Ringer's in the presence of mucosal amiloride), our mean values for α and fR_a are 15 ± 2 (n = 17) and 0.92 ± 0.01, respectively. Using DC microelectrode techniques, Nagel et al. (1981) measured fR_a under similar conditions and report a mean value of 0.91 ± 0.01 (n = 13). This value is statistically indistinguishable from our impedance-determined value (P = 0.6, by unpaired t-test), supporting the notion that G_j is small compared to the transcellular conductance. Because of comparable magnitudes of R_b and R_p (*see below*), α is significantly lower than R_a/R_b (mean value of 19 ± 3).

For an epithelium possessing finite G_j, fitting the impedance data by a model which assumes that G_j equals zero will yield incorrect estimates of the other parameters. As discussed above, one result would be an impedance-predicted resistance ratio α

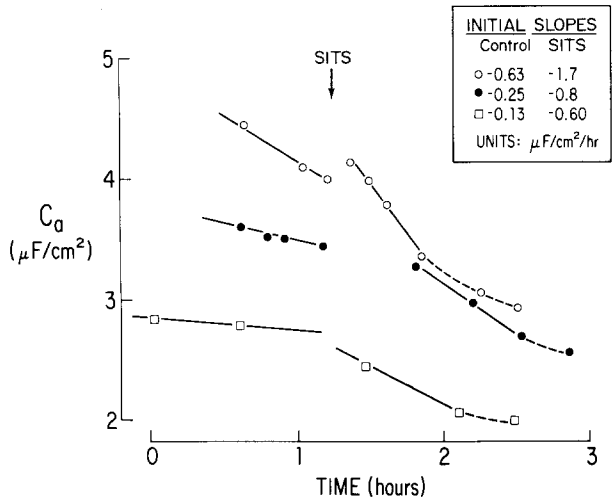

Fig. 3. C_a plotted as a function of time measured in three different tissues. Sodium transport was inhibited with mucosal amiloride and serosal ouabain, and proton transport was inhibited by the addition of SITS (arrow)

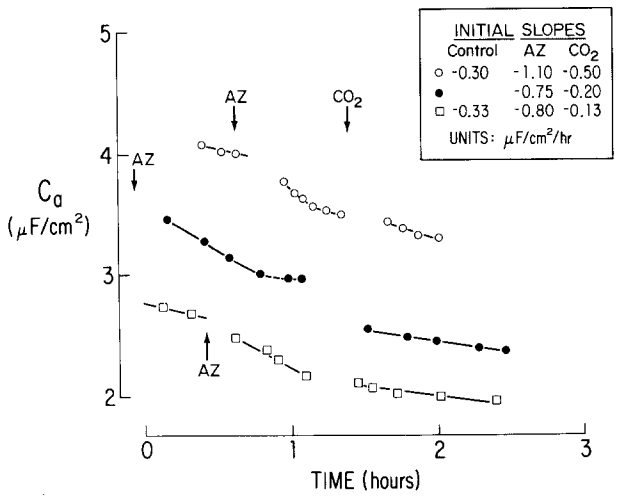

Fig. 4. C_a plotted as a function of time measured in three different tissues. Sodium transport was inhibited using mucosal amiloride and serosal ouabain, and proton transport was inhibited by the addition of AZ (arrow marked *AZ*). Proton secretion was reduced by washing the serosal side with solution containing CO_2 and HCO_3^- (arrow marked *CO_2*)

that exceeds the true value measured using microelectrodes. The agreement between the impedance and microelectrode measurements presented above supports the notion that in turtle bladder, G_j is small compared to the transcellular conductance. However, questions still remain as to the effect of a small finite G_j on the determination of the other parameters.

We investigated this question by assigning a value of G_j equal to 20% of the transepithelial conductance, and subsequently reanalyzing the impedance in order to determine how this altered the estimates of the other model parameters. This analysis was done in two representative tissues which possessed markedly different membrane resistance ratios (R_a/R_b equal to 14 and 43, respectively, as determined by the initial analyses with G_j equal to zero). Determinations of C_a, C_b, and R_p were found to be insensitive to G_j, differing by an average of 1.9% (range 0 to 4.6%) from the previous estimates where G_j was equal to zero. Determinations of G_a and G_b differed by an average of 14% (range 3 to 19%) from the previous estimates. We therefore conclude that even if the bladder possesses a substantial paracellular conductance, our analysis will result in uncertainties only in G_a and G_b.

Membrane-Capacitances in Ouabain-Treated Bladders

Under control conditions where the tissue was treated with ouabain and amiloride, the apical membrane capacitance C_a initially averaged 3.7 ± 0.7 μF/cm² (n = 9), which implies that microvilli and folding of the apical membrane result in a 3.7-fold increase in membrane area over nominal chamber area, assuming a membrane specific capacitance of 1 μF/cm². Moreover, the capacitance ratio C_a/C_b was 0.46 ± 0.04 (n = 9), implying that the basolateral membrane area was 2.2 times greater than the apical area. Micrographs show more basolateral membrane area than apical membrane area, hence this finding is not unexpected.

C_a was found, however, to decrease continually over time under control conditions. Moreover, application of SITS, an irreversible inhibitor of proton transport which reduced I_{sc} from −10 ± 2 to −1.3 ± 0.6 μA/cm² (n = 4), accelerated the initial rate of decline in C_a. These results are shown in Fig. 3. Under control conditions, C_a decreased at a rate of −0.35 ± 0.11 μF/(cm² hr). Initially following applications of SITS, the rate of decline was doubled to −0.73 ± 0.11 μF/(cm² hr), but over time (*ca.* 1 hr) the rate of decline appeared to return to the control level. The basolateral membrane capacitance C_b also continually decreased with time, but SITS did not affect its rate of decline.

A similar response was also observed in bladders using 50 μM AZ to inhibit transport reversibly, and this is shown in Fig. 4. Under control conditions, I_{sc} was −8.5 ± 1.4 μA/cm² (n = 5) and C_a declined at a rate of −0.68 ± 0.25 μF/(cm² hr). Following the application of AZ, I_{sc} decreased to −3.7 ± 1.0 μA/cm² and the initial rate of decline in C_a was accelerated to −1.0 ± 0.4 μF/(cm² hr). Finally,

Table 1. Effect of removal of albumin from the serosal bathing solution[a]

	G_a (mS/cm²)	C_a (μF/cm²)	G_b (mS/cm²)	C_b (μF/cm²)	R_p (Ω cm²)
Control	0.34 ± 0.04	3.8 ± 0.8	4.6 ± 0.7	8.8 ± 0.8	290 ± 88
No albumin	0.37 ± 0.03	3.8 ± 0.8	5.7 ± 0.8	11.3 ± 1.5	214 ± 44
P	NS	NS	0.003	0.02	NS

[a] The first row shows mean values (± SEM) from eight bladders bathed with serosal solution containing 2% albumin. The second row shows mean values obtained from the same bladders after removal of the serosal albumin. The probabilities were obtained using a paired *t*-test. Probabilities greater than 0.05 were considered not significant (NS).

restimulation of proton transport by washing the serosal chamber with CO_2 and HCO_3^--containing solutions (*see* Materials and Methods) resulted in an increase in I_{sc} to -9.9 ± 1.3 μA/cm² and a reduction in the rate of decline in C_a to -0.35 ± 0.15 μF/(cm² hr). Again, C_b was observed to decline in these experiments, but its rate of decline was not dependent on the proton transport rate.

I_{sc} appeared stable prior to inhibition by SITS and AZ, and after maximum inhibition was achieved. These data indicate that changes in the rate of proton transport are associated with changes in C_a, since the initial rate of decline of C_a accelerates after application of the inhibitors. However, in these experiments, we never observed a true increase in C_a upon stimulation of transport, as might be expected from micrographic observations (Stetson & Steinmetz, 1983).

Membrane-Resistances in Ouabain-Treated Bladders

The apical and basolateral resistances (R_a and R_b, respectively) also increased with time concomitant with the changes observed in the membrane capacitances. This confirms that in bladders treated with ouabain and amiloride, a continual decrease in membrane area occurs; the observed changes in the capacitances cannot be explained by changes in the membrane specific capacitances.

Inhibition of transport produced additional changes in the membrane resistances that could not be explained alone by the reduction of exposed membrane. For example, in the SITS experiments discussed above, R_a increased from 3.9 ± 1.1 to 6.7 ± 1.2 kΩ cm² after maximum inhibition was achieved. Using C_a to normalize the resistance to unit area of apical membrane, we found that the apical membrane specific resistance increased from 13 ± 2 to 17 ± 2 kΩ μF, reflecting a modest decrease in the apical membrane ionic conductance thereby suggesting a decrease in the membrane permeability. On the other hand, R_b was independent of the transport rate and exhibited a mean value of 240 ± 19 Ωcm² ($n = 8$). Using C_b to normalize this value to actual membrane area resulted in a basolateral membrane specific resistance of 1.6 ± 0.14 kΩ μF.

Membrane Area Changes Unrelated to Proton Transport

The results just presented demonstrate that changes in the rate of proton transport can be temporally associated with changes in the apical membrane capacitance, and hence area. However, the results also reveal that under the conditions imposed (i.e., treatment with ouabain and amiloride), the tissue exhibits a decline in both apical and basolateral capacitance that is unrelated to the proton transport rate. This continual decline of these parameters over time precludes quantification of the magnitude of change in surface area that might be related to proton transport. Furthermore, attempts to characterize the kinetics of transport-related changes in capacitance would be confounded by the presence of the changing base line. For these reasons, we decided to investigate the cause of the transport-independent decline in capacitance.

We postulated that the transport-independent changes in C_a and C_b could occur as a result of slow changes in cell volume during the course of each experiment, since changes in cell volume could affect membrane capacitance, either by exposing cell membrane that had been pinched off or tightly infolded, or by affecting the rate of either vesicle fusion or vesicle retrieval from the plasma membrane. Since the experiments were performed in the presence of ouabain, we thought it possible that the cells' ability to regulate their volume may have been hampered. In addition, it has been reported that serum proteins facilitate fluid transport across the basolateral membrane (Grantham et al., 1972). Since the serosal bathing solution was devoid of protein, we thought it possible that this too might affect the cells' ability to volume regulate.

Table 2. Effect of addition of nystatin to the mucosal bathing solution[a]

	G_a (mS/cm²)	C_a (μF/cm²)	G_b (mS/cm²)	C_b (μF/cm²)	R_p (Ω cm²)
Control	0.27 ± 0.05	2.0 ± 0.2	4.9 ± 0.7	6.0 ± 0.7	294 ± 78
Nystatin	1.08 ± 0.27	3.2 ± 0.6	0.89 ± 0.31	10.1 ± 1.8	544 ± 76
P	0.02	0.03	0.001	0.02	<0.001

[a] The first row shows mean values from five bladders in normal Ringer's solution. The second row shows mean values obtained from the same bladders after addition of the nystatin. In four of the five bladders, the serosal bathing solution contained 2% albumin. The probabilities were obtained using a paired t-test.

In order to investigate the hypothesis that cell volume changes were responsible for the transport-independent changes in the membrane capacitances, we measured impedance from bladders where ouabain was omitted from the serosal solution. Instead, we used only mucosal amiloride to inhibit sodium transport, thereby leaving the Na,K-ATPase functional. In addition, we added 2% albumin to the serosal solution. We found that under these conditions, all circuit parameters remained stable with time.

Subsequent removal of albumin from the serosal bathing solution resulted in an increase in C_b and the basolateral conductance G_b, although the other circuit parameters remained essentially unchanged, and these results are summarized in Table 1. The percent increases in C_b and G_b (28 ± 11% and 30 ± 8%, respectively) were found to be identical (P = 0.9 by paired t-test). Hence there was no change (P = 0.8) in the normalized basolateral conductance (conductance divided by the capacitance as representative of the membrane area) which was 0.55 ± 0.11 mS/μF under control conditions, and 0.56 ± 0.11 mS/μF after albumin removal. This result indicates that albumin removal results solely in an increase in basolateral membrane area, with no change in the specific conductances of that membrane.

To test further our hypothesis that changes in cell volume result in changes in membrane area, we used the ionophore nystatin to induce cell swelling. Nystatin is a polyene antibiotic which forms ionic channels in membranes that are permeable to both cations and anions (Lewis et al., 1977). When added to the mucosal bathing solution, one expects an influx of both sodium and chloride coupled with an efflux of intracellular potassium. The NaCl influx is expected to result in an osmotically induced water influx, thereby resulting in cell swelling. The results of these experiments are summarized in Table 2. Application of mucosal nystatin resulted in a dramatic increase in the apical membrane conductance G_a, as expected, due to the increased apical membrane ionic permeability. In addition, G_b decreased dramatically, which is also expected. Since the basolateral membrane is known to be highly potassium permeable (Nagel et al., 1981), the nystatin-induced decrease in intracellular potassium results in the measured decrease in the basolateral membrane's conductance. Cell swelling after nystatin addition is also supported by the fact that the lateral space path resistance R_p nearly doubled. Cell swelling is expected to reduce the width of the lateral spaces, thereby decreasing their cross-sectional area and hence increasing R_p. Finally, C_a and C_b also increased after nystatin application, thereby providing support for the notion that cell swelling results in increases in membrane area. A representative experiment showing the rapid increase in C_a and C_b following the addition of nystatin is shown in Fig. 5. This figure also demonstrates the stability of C_a and C_b during the base-line period which is achieved when bladders are bathed in an albumin-containing bath and sodium transport is inhibited using amiloride.

Membrane Parameters Under Control Conditions

The findings just presented support the notion that the apparent decline in membrane area with time, as noted in our initial experiments, is related to changes in cell volume. Moreover, stabilization of membrane circuit parameters could be achieved by studying the bladder under conditions designed to minimize these volume changes. The mean base-line parameters are summarized in Table 3 and were measured under conditions where the serosal solution contained 2% albumin, and sodium transport was inhibited using only mucosal amiloride. The results presented below are from bladders that were initially under these conditions.

Series Resistance

The average series resistance (R_s) was 147 ± 5 Ωcm² (n = 17) and simply reflects the finite resis-

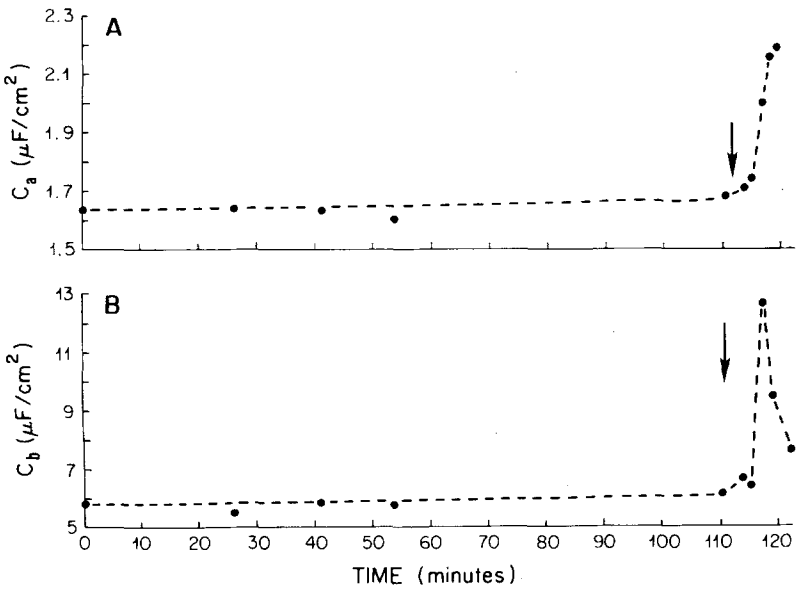

Fig. 5. C_a (panel *A*) and C_b (panel *B*) in a single bladder plotted as a function of time. Sodium transport was inhibited using mucosal amiloride. 2% BSA was included in the serosal solution. After an initial base-line period of observation, nystatin (arrow) was added to the mucosal solution and its effect on C_a and C_b noted

Table 3. Mean parameter values from 17 bladders under control conditions[a]

Model Parameters:				
G_a (mS/cm^2)	C_a (μF/cm^2)	G_b (mS/cm^2)	C_b (μF/cm^2)	R_p (Ω cm^2)
0.30 ± 0.03	3.2 ± 0.4	4.9 ± 0.6	8.2 ± 0.9	256 ± 49
Computed Parameters:				
R_a/R_b	C_a/C_b	$G_{a\text{-norm}}$ (mS/μF)	$G_{b\text{-norm}}$ (mS/μF)	
—	—			
19 ± 3	0.40 ± 0.04	0.11 ± 0.01	0.64 ± 0.07	

[a] Sodium transport was inhibited using mucosal amiloride, and the serosal bathing solution contained 2% albumin. The normalized conductances were computed as the ratio of the conductance to the capacitance of each respective membrane.

tance of the solution between the voltage-measuring electrodes and the apical and basolateral surfaces. R_s varies with the separation of the voltage electrodes and the bulk solution resistivity, but would not be expected to vary measurably with changes in the rate of epithelial transport.

Effects Resulting from Changes in the Proton Transport Rate

We showed earlier that alterations in proton transport rate results in changes in membrane parameters, notably in the apical capacitance. However, recall that those results were obtained from tissues exhibiting unstable base lines. In order to investigate the effects of alterations in stable bladders, the following experiments were done.

Table 4 shows results obtained in seven bladders where transport was initially inhibited using 50 μM AZ, followed by restimulation of proton transport by washing the serosal chamber with solution containing CO_2 and HCO_3^-. Under control conditions, I_{sc} was -4.3 ± 0.5 μA/cm^2, and decreased to -1.4 ± 0.6 μA/cm^2 after AZ. Associated with this decline in transport was a small but significant change in C_a which decreased by an average of 8.2 ± 1.3%. We also observed a significant decrease in G_a. This did not, however, represent a measurable change in the specific conductance of the apical membrane since its normalized conductance did not change (0.090 ± 0.009 mS/μF before AZ, and 0.081 ± 0.010 mS/μF after AZ, $P = 0.08$ determined by a paired *t*-test). None of the other membrane parameters changed with AZ treatment, indicating that the effect observed was specific to the apical membrane.

Upon washing the serosal bath with solution containing CO_2 and HCO_3^-, I_{sc} increased to -4.4 ± 0.9 μA/cm^2. C_a returned to a value indistinguishable from control values. G_a also increased significantly, but this increase was not fully explained by the increase in C_a since the normalized conductance of the apical membrane was also found to increase significantly (to 0.097 ± 0.013 mS/μF, $P = 0.01$ compared to during AZ treatment). We suspect that this small increase in the normalized apical conductance reflects a HCO_3^- conductance (Satake et al., 1983) or a Cl^- conductance. In addition to the changes in the apical membrane parameters, changing to the CO_2 and HCO_3^--containing solution was associated with a small but significant decline in C_b. This decline in C_b was not accompanied by changes in G_b. Moreover, the normalized conductance of the basolateral membrane did not change significantly (0.66 ± 0.11 mS/μF before solution change, 0.70 ± 0.13

Table 4. Effect of inhibiting proton transport in seven bladders using AZ, with subsequent restimulation of transport with CO_2 and HCO_3^-[a]

	G_a (mS/cm²)	C_a (μF/cm²)	G_b (mS/cm²)	C_b (μF/cm²)	R_p (Ω cm²)
Control	0.26 ± 0.05	2.9 ± 0.4	5.3 ± 1.2	8.2 ± 1.2	163 ± 29
50 μM AZ	0.22 ± 0.04	2.7 ± 0.4	5.3 ± 1.4	8.4 ± 1.8	169 ± 31
P	0.02	0.002	NS	NS	NS
$CO_2 + HCO_3^-$	0.27 ± 0.05	2.8 ± 0.4	4.9 ± 1.3	7.4 ± 1.6	187 ± 36
P	0.003	0.02	NS	0.03	0.04

[a] The first row shows mean parameter values under control conditions. The second row shows values measured from the same bladders after the addition of AZ. The third row shows probabilities (paired *t*-test) comparing the control and AZ values. The fourth row shows values from the same bladders after restimulation of transport with CO_2 and HCO_3^-. The last low shows probabilities comparing the AZ and $CO_2 + HCO_3^-$ values.

after, $P = 0.08$ determined by paired *t*-test). Although this change in solution enhanced proton transport, and it is known that increasing the serosal HCO_3^- concentration increases the rate of HCO_3^-/Cl^- exchange in the bladder (Leslie et al., 1973), we cannot be sure that this change in C_b is in fact related to changes in ion transport. Further studies are necessary to clarify the physiological significance of this finding. Finally, we noted a small significant increase in the lateral space path resistance (R_p). This increase could be explained by either slight cell swelling in the presence of HCO_3^--containing solution resulting in narrowing of the lateral spaces, or to small changes in the resistivity of the solution filling the lateral spaces.

These data show that CO_2/HCO_3^--induced increases in the proton transport rate result in small but measurable increases in C_a, and hence apical membrane area. Moreover, we observe a concomitant increase in G_a caused in part by the change in membrane area, but also reflecting measurable changes in the specific conductance of the membrane.

Discussion

Single-Cell Model

The equivalent-circuit model used in this study was one that was originally derived in studies of mammalian urinary bladder (Clausen et al., 1979). Mammalian urinary bladder has a simpler structure than turtle bladder in that it possesses only one functional cell type (Lewis & Diamond, 1976). Turtle bladder, on the other hand, possesses two major cell types. Mitochondria-rich cells make up approximately 10 to 20% of the total cell number and are believed to be solely responsible for electrogenic proton secretion (Schwartz et al., 1982). Granular cells make up about 75% of the epithelial cell number and are thought to mediate sodium transport (Schwartz et al., 1972). If these two cell types possessed different membrane properties, or if they were not coupled to one another by low-resistance pathways, then one would not expect that the distributed model would be capable of accurately representing the measured impedance (*cf.* Clausen et al., 1983).

Quite surprisingly, we found the contrary. The distributed model fits the measured impedance with exceptional accuracy, exhibiting no consistent deviations in the fits that could be attributed to two different populations of cells. Several lines of evidence indicate that the parameter estimates arising from fits by the model reflect mean properties of the two cell types. The base-line value for C_a indicates that the apical membrane area is nominally 3.2 times higher than the chamber area. If C_a reflected solely the area of the mitochondira-rich cell population, then one would expect to measure a much smaller value owing to the small cell number. On the other hand, if C_a only reflected the capacitance of the granular cells, then one would not expect to observe proton transport-related changes in its value, since the maneuvers used are known to be selective for the mitochondria-rich cells (Husted et al., 1981; Stetson & Steinmetz, 1983). We obtain even stronger evidence that the parameters reflect mean tissue properties when we consider the magnitude of the transport-related changes in C_a. Stimulation of proton transport has been shown in micrographic studies to result in a twofold increase in the apical membrane area of only mitochondria-rich cells (Stetson & Steinmetz, 1983). Considering their relative cell number, this would correspond to a 5 to 20% increase in the apical membrane area of the whole epithelium. We observe an 8.2% change in C_a with changes in proton transport, which is consis-

tent with the notion that we are measuring mean properties of the whole epithelium.

Since it appears that the measured parameters represent mean properties of the two cell types, this tacitly implies that the two cell types are electrically coupled to some degree. This is perplexing at best since the existence of gap junctions between the cell types has not been reported. Nevertheless, other evidence has been reported that supports the notion of electrical coupling. Microelectrode studies have been performed in turtle bladder (Nagel et al., 1981), but in these studies no mention was made of two distinct populations of cells possessing different properties. In addition, mucosal amiloride (0.1 mM) is known to inhibit proton transport to some extent, and this effect can be prevented by treatment with serosal ouabain (Husted & Steinmetz, 1979). If one assumes that these two agents act selectively on the granular cells (Schwartz et al., 1982), then an explanation of their effects on proton transport could involve electrical coupling.

Cell Volume Changes

The results from our nystatin studies indicate that maneuvers designed to induce cell swelling result in increases in membrane capacitances, and hence membrane areas. Because these maneuvers caused increases in intracellular NaCl, and decreases in intracellular potassium, we suspect that the changes in area reflect a regulatory mechanism involving addition of pumps and/or channels necessary for maintenance of normal cell volume. It is of interest in this regard that Warncke and Lindemann (1981) found that treatment of epithelial cells with vasopressin resulted in increases in apical and basolateral capacitance. The increase in apical capacitance is most likely related to vasopressin-induced fusion of tubulo-vesicle structures with the apical membrane. Since treatment with vasopressin is also associated with cell swelling (DiBona et al., 1969), it is distinctly possible that this triggers vesicle fusion with the basolateral membrane, and thus the increase in C_b noted in those studies.

Since we found similar changes in membrane capacitances in our earlier studies where serosal ouabain was used to inhibit sodium transport, and where the serosal bathing solution was hypo-oncotic, we suspect that they are also related to cell volume changes. It is interesting to note that the slow continual decreases in membrane area with time, observed under these conditions, were not accompanied by changes in the rate of proton transport. This suggests the existence of more than one class of transport-related processes involving endocytosis and exocytosis, where the mechanism involving volume regulation might involve membrane which is relatively devoid of proton pumps.

Transport-Related Changes in Membrane Parameters

The results have shown that impedance-analysis techniques are capable of quantifying changes in the electrophysiological parameters that are related to proton transport. We find that reducing the rate of proton transport with AZ results in no change in the basolateral membrane area or specific conductance, confirming that the species transported across that membrane do so via electrically silent pathways. Changes in the rate of transport involving a Cl^-/HCO_3^- exchange process (Fischer, Husted & Steinmetz, 1983) would not be expected to cause a detectable change in the specific conductance of the membrane.

The changes noted in the apical membrane capacitance following AZ treatment are consistent with the notion that AZ inhibits proton transport at least in part by reducing the number of apical membrane proton pumps. This reduction could be due to changes in the rates of endocytosis and/or exocytosis. A more detailed examination of this process is currently in progress in this laboratory.

Stimulation of proton transport with CO_2 and HCO_3^- caused not only the increase in C_a which is expected if membrane fusion is an important mechanism of the stimulation, but also an increase in the specific conductance of the apical membrane. This specific conductance increase could represent addition of Cl^-- or HCO_3^--conductive channels in parallel with the addition of pumps, or could simply reflect the alteration of electrochemical gradients (e.g., Cl^- and HCO_3^-) across the apical membrane. Since the small transepithelial currents used to measure the impedance are not expected to alter the proton pump current, we do not feel that the proton pump contributes directly to G_a.

The decrease in C_b after stimulation of proton transport is puzzling. At this time, we have no explanation of this result, nor do we have any evidence that this is directly related to the regulation of transport.

Conclusions

We conclude from these studies that the analysis of transepithelial impedance accurately quantifies the different membrane electrical characteristics. Moreover, by measuring the different membrane

capacitances, we can obtain estimates of the membrane areas, thereby allowing us to monitor changes in the net rates of endocytosis and exocytosis that are associated with changes in the rate of proton transport. These techniques provide a valuable tool for studying the mechanism of proton transport in relation to membrane conductances and electrochemical gradients, the regulation of the rate of proton transport resulting from changes in membrane conductance and endocytosis and exocytosis, and the kinetic interrelationships of these parameters.

This work was supported by NIH grants AM 30394 and AM 28074. T.D. was a Research Associate of the Veterans Administration while some of these studies were in progress. A portion of this work has been published previously (*see* Clausen & Dixon, 1984).

References

Clausen, C., Dixon, T., 1984. Membrane area changes associated with proton secretion in turtle urinary bladder studied using impedance analysis techniques. *In:* Current Topics in Membranes and Transport. A. Kleinzeller and F. Bronner, editors. Vol. 20, pp. 47–60. Academic, New York.

Clausen, C., Fernandez, J.M. 1981. A low-cost method for rapid transfer function measurements with direct application to biological impedance analysis. *Pfluegers Arch.* **390:**290–295

Clausen, C., Lewis, S., Diamond, J.M. 1979. Impedance analysis of a tight epithelium using a distributed model. *Biophys. J.* **26:**291–317

Clausen, C., Machen, T.E., Diamond, J.M. 1983. Use of AC impedance analysis to study membrane changes related to acid secretion in amphibian gastric mucosa. *Biophys. J.* **41:**167–178

Clausen, C., Reinach, P.S., Marcus, D.C. 1986. Membrane transport parameters in frog corneal epithelium measured using impedance analysis techniques. *J. Membrane Biol.* **91:**213–225

Clausen, C., Wills, N.K. 1981. Impedance analysis in epithelia. *In:* Ion Transport by Epithelia. S.G. Schultz, editor. pp. 79–92. Raven, New York

Cole, K.S. 1972. Membranes, Ions and Impulses. University of California Press, Berkeley

Diamond, J.M., Machen, T.E. 1983. Impedance analysis in epithelia and the problem of gastric acid secretion. *J. Membrane Biol.* **72:**17–41

DiBona, D.R., Civan, M.M., Leaf, A. 1969. The cellular specificity of the effect of vasopressin on toad urinary bladder. *J. Membrane Biol.* **1:**79–91

Fischer, J.L., Husted, R.F., Steinmetz, P.R. 1983. Chloride dependence of the HCO_3^- exit step in urinary acidification by the turtle bladder. *Am. J. Physiol.* **245:**F564–F568

Gluck, S., Cannon, C., Al-Awqati, Q. 1982. Exocytosis regulates urinary acidification in turtle bladder by rapid insertion of H^+ pumps into the luminal membrane. *Proc. Natl. Acad. Sci. USA* **79:**4327–4331

Grantham, J.J., Qualizza, P.B., Welling, L.W. 1972. Influence of serum proteins on net fluid reabsorption of isolated proximal tubules. *Kidney Int.* **2:**66–75

Husted, R.F., Mueller, A.L., Kessel, R.G., Steinmetz, P.R. 1981. Surface characteristics of the carbonic-anhydrase-rich cells in the turtle urinary bladder. *Kidney Int.* **19:**491–502

Husted, R.F., Steinmetz, P.R. 1979. Effect of amiloride and ouabain on urinary acidification by turtle bladder. *J. Pharmacol. Exp. Ther.* **210:**264–268

Leslie, B.R., Schwartz, J.H., Steinmetz, P.R. 1973. Coupling between Cl^- absorption and HCO_3^- secretion in turtle urinary bladder. *Am. J. Physiol.* **225:**610–617

Lewis, S.A., Diamond, J.M. 1976. Na^+ transport by rabbit urinary bladder, a tight epithelium. *J. Membrane Biol.* **28:**1–35

Lewis, S.A., Eaton, D.C., Clausen, C., Diamon, J.M. 1977. Nystatin as a probe for investigating the electrical properties of a tight epithelium. *J. Gen. Physiol.* **70:**427–440

Nagel, W., Durham, J.H., Brodsky, W.A. 1981. Electrical characteristics of the apical and baso-lateral membranes in the turtle bladder epithelial cell layer. *Biochim. Biophys. Acta* **646:**78–87

Reeves, W.S., Gluck, S., Al-Awqati, Q. 1983. Role of endocytosis in H^+ secretion regulation by turtle bladder. *Kidney Int.* **23:**237

Rosen, S. 1970. The turtle bladder. I. Morphological studies under varying conditions of fixation. *Exp. Mol. Pathol.* **12:**286–296

Satake, N., Durham, J.H., Ehrenspeck, G., Brodsky, W.A. 1983. An electrogenic mechanism for alkalai and acid transport in turtle bladders. *Am. J. Physiol.* **244:**C259–C269

Schwartz, J., Bethencourt, D., Rosen, S. 1982. Specialized functions of carbonic-anhydrase-rich and granular cells of turtle bladder. *Am. J. Physiol.* **242:**F627–F633.

Schwartz, J.H., Rosen, S., Steinmetz, P.R. 1972. Carbonic anhydrase function and the epithelial organization of H^+ secretion in turtle urinary bladder. *J. Clin. Invest.* **51:**2652–2662

Steinmetz, P.R. 1974. Cellular mechanisms of urinary acidification. *Physiol. Rev.* **54:**890–956

Stetson, D.L., Beauwens, R., Palmisano, J., Mitchell, P.P., Steinmetz, P.R. 1985. A double-membrane model for urinary bicarbonate secretion. *Am. J. Physiol.* **249:**F546–F552

Stetson, D.L., Steinmetz, P.R. 1983. Role of membrane fusion in CO_2 stimulation of proton secretion by turtle bladder. *Am. J. Physiol.* **245:**C113–C120

Warncke, J., Lindemann, B. 1981. Effect of ADH on the capacitance of apical epithelial membranes. *Proc. Adv. Physiol. Sci.* **3:**129–133

Received 24 October 1985; revised 19 February 1986